

K.J. Orlik-Rückemann and E.S. Hanff,
Unsteady Aerodynamics Laboratory,
National Aeronautical Establishment,
National Research Council of Canada,
Ottawa, Ontario, Canada.

ABSTRACT

A review is presented of some of the fluid dynamics phenomena that are associated with oscillatory flight at high angles of attack, with particular emphasis on asymmetric shedding of forebody vortices, asymmetric breakdown of leading edge vortices, the oscillatory motion of such vortices, and the time lag between the vortex motion and the causative motion of the aircraft. These phenomena cause a number of important effects on the dynamic stability parameters at high α , such as strong non-linearities with α , significant static and dynamic aerodynamic cross coupling, large time-dependent effects and a strong configuration dependence. New wind tunnel testing techniques to determine all the required direct, cross and cross-coupling moment derivatives due to oscillation in pitch, yaw and roll as well as in vertical and lateral translation are briefly described.

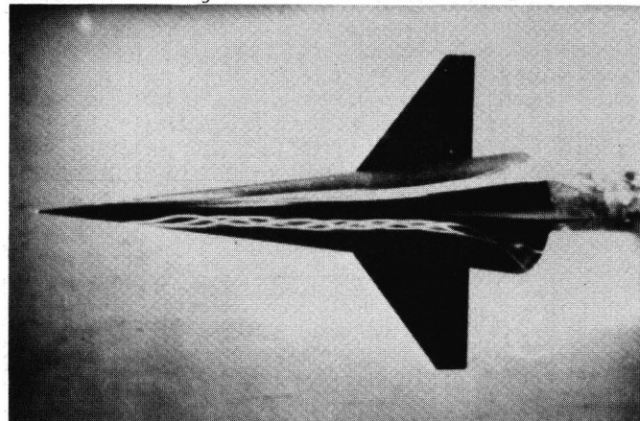
1. INTRODUCTION

The advent of flight at high angles of attack has revived our interest in dynamic stability of aircraft and missiles. In this paper some of the fluid dynamics phenomena occurring at high angles of attack will be reviewed, with particular attention to phenomena associated with oscillatory flows. The effects of these phenomena on various dynamic stability parameters will be discussed, using experimental data obtained from oscillatory wind-tunnel tests. The special experimental techniques developed for these tests will be described, with particular emphasis on equipment and methods recently introduced at the National Aeronautical Establishment. The effect of including, in the equations of motion of an aircraft, the various dynamic stability parameters that are characteristic of flight at high angles of attack will be illustrated by examples of an appropriate sensitivity study.

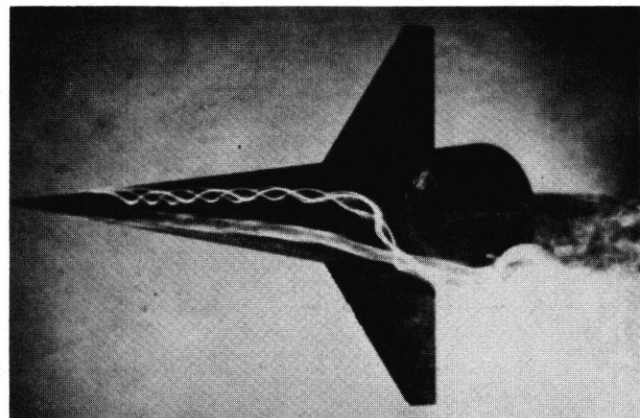
2. SOME FLUID DYNAMICS PHENOMENA AT HIGH ANGLES OF ATTACK

Of the many flow phenomena occurring at higher angles of attack, probably the most important ones are associated with the formation of forebody vortices and their asymmetric shedding when the angle of attack reaches a certain threshold value.

These phenomena are of particular interest for missiles and for modern fighter aircraft, which often feature long slender fuselages with a high forebody fineness ratio. Although a large number of investigations have been conducted in this area in recent years^(1,2), the analytical prediction of such flow fields is not yet generally possible and the determination of the resulting aerodynamic characteristics has therefore to be based on experiments for some time to come. Such experiments have so far mainly consisted of various types of static wind-tunnel tests and are often reinforced by flow visualization studies carried out in water tunnels (Fig. 1). These studies can frequently provide valuable insight in the rather complex



(a) Symmetric vortices; $\alpha = 25^\circ$



(b) Asymmetric vortices; $\alpha = 45^\circ$

Figure 1. Flow visualization in NAE Water Tunnel.

three-dimensional flow fields occurring at high angles of attack. It has been found that the forebody vortex system is affected by the nose geometry such as represented by the cross-section shape, bluntness and fineness ratio and that, for a given geometry, the angle of attack for the onset of asymmetry, α_0 , is a strong function of the semiapex angle of the nose, δ_N . For pointed forebodies of circular cross-section this function is approximately $\alpha_0 \approx 2 \delta_N$ (3).

Another flow phenomenon that is important at higher angles of attack is the breakdown of vortices formed at the leading edge of the wing. This vortex burst is highly dependent on the leading edge sweep. For a delta wing, the angle of attack at which vortex breakdown occurs at the wing trailing edge increases approximately linearly with the leading edge sweep (4), as shown in Fig. 2, where the different points represent values obtained both in air and in water and at Reynolds numbers in the range $1.5 \cdot 10^4$ to $2 \cdot 10^6$. As the angle of attack increases further, the breakdown occurs gradually more and more forward of the trailing edge. For highly swept delta wings the vortex burst location may become asymmetric (4,5), causing an onset of asymmetric aerodynamic reactions in a manner which appears analogous to the effects of forebody vortex asymmetry, discussed before (Fig. 3). It is interesting to note that in both cases the height of the vortex core above the surface of the wing (or of the body) also becomes markedly different between the right and the left side of the configuration in question.

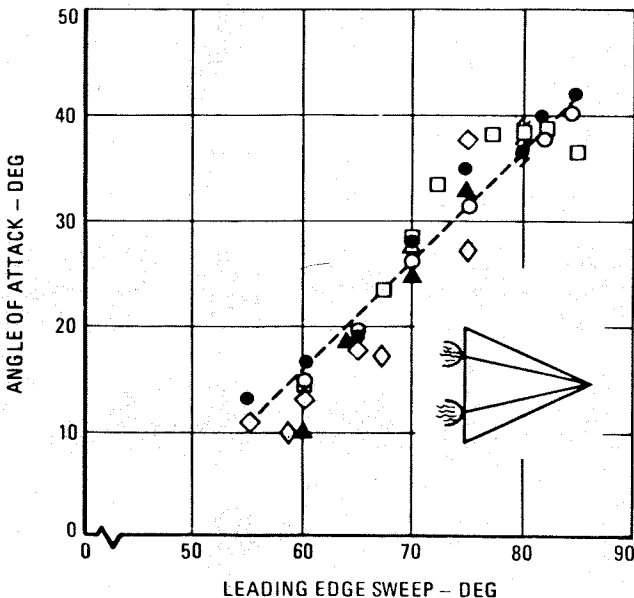


Figure 2. Onset of vortex breakdown at the trailing edge of a delta wing (obtained in air and in water at $1.5 \cdot 10^4 < Re < 2 \cdot 10^6$). (Ref. 4)

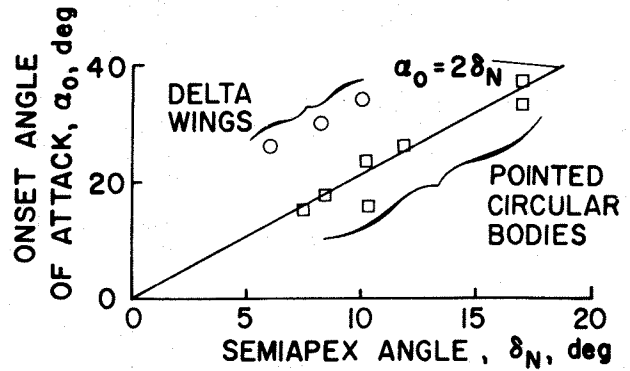


Figure 3. Onset of asymmetry for pointed circular forebodies (side force) and delta wings (rolling moment). (Refs. 4 and 5)

The flow phenomena about highly swept wings are similar to those occurring on the so-called wing leading-edge extensions (LEX) or wing-body strakes. On an aircraft configuration large interactions may occur between the forebody vortices and the vortex systems emanating from the leading edges of the various wing surfaces. If the vortex breakdowns or the asymmetric vortices are located close to any stabilizing or control surfaces of the aircraft, significant effects on aerodynamic reactions may result.

Forebody vortices and leading edge vortices are examples of fluid dynamics phenomena that vary significantly with angle of attack and that at high enough values of that parameter may cause asymmetric effects, even if the aircraft itself continues to head symmetrically into the wind (i.e. has zero sideslip). Other such phenomena may also be envisaged, such as may be caused by flow separation or boundary layer transition on wings and control surfaces. Although also important, such additional phenomena have a more local effect that those mentioned before and are therefore of less importance in the present context.

The phenomena listed so far, of course, are not necessarily associated with dynamic flight conditions but occur in both steady and oscillatory flows. What makes the oscillatory flows particularly involved is the introduction of the time element into this already rather complex picture. The forebody vortices change their lateral and vertical positions as functions of angle of attack, which itself is a function of time. So does the longitudinal location of "fully developed" leading-edge vortex bursts. The various components of the aircraft, such as the fin and the horizontal stabilizer, move in and out of local flow regions in which they are embedded. To make matters even more complex, all these motions take place not in a manner simultaneous with the motion of the aircraft, but with a certain delay, mainly due to the

convective time lag. The delay is a function of the distance of the station under consideration from the station at which a particular flow phenomenon, such as a vortex, leaves the surface of the aircraft. This is demonstrated clearly on the flow visualization motion pictures made in the NAE water tunnel, and shown during the oral presentation. Thus aerodynamic reactions that have components both in-phase and out-of-phase with the motion of the aircraft can be expected to materialize.

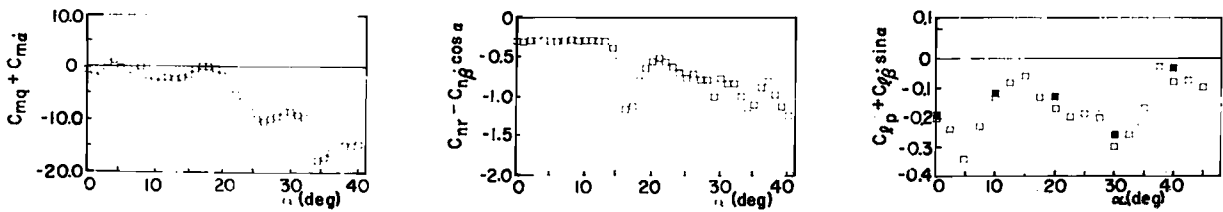
It should be noted, that although for an aircraft flying at high angle of attack asymmetric flow may occur even at zero nominal sideslip (as discussed above), such an asymmetric flow will also occur, of course, at lower angles of attack when the aircraft is exposed to finite angles of sideslip. Since such a flight condition is encountered quite frequently, the remarks in this paper that deal with the effects of flow asymmetries have a rather general application. It should also be mentioned, that the phenomenon of vortex burst is quite sensitive to the sweep angle of the wing and therefore is also strongly dependent on the angle of sideslip. For

instance, even if an aircraft flies at an angle of attack below vortex burst, an oscillatory variation in the instantaneous angle of sideslip may, under some circumstances, cause a corresponding periodic occurrence of the vortex bursts on the wings. High angle of attack, therefore, is to some extent equivalent to a combination of a somewhat lower angle of attack and a finite angle of sideslip, and these two flight conditions will be considered together in the remaining part of this paper.

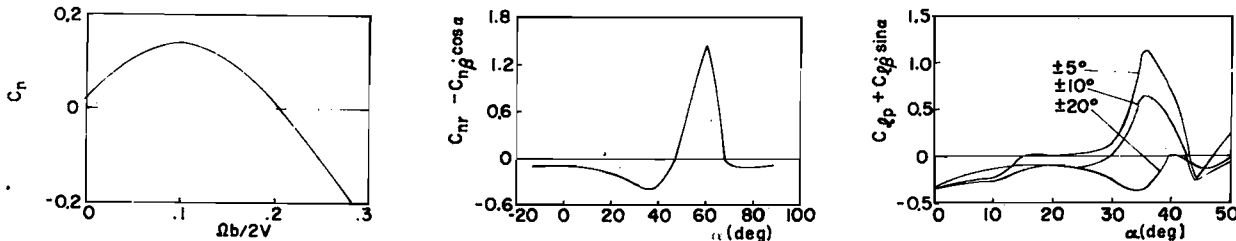
3. EFFECTS OF HIGH- α FLOW PHENOMENA ON DYNAMIC STABILITY PARAMETERS

The aforementioned flow phenomena have large effects on all the aerodynamic characteristics of the aircraft including, of course, the static and dynamic stability parameters. For dynamic stability considerations, which are the subject of this paper, the most important such effects are (6)

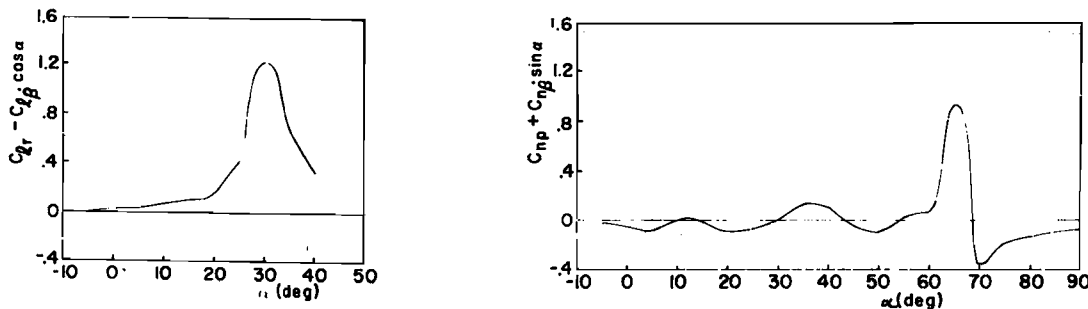
- large non-linear variations of stability parameters with the angle of attack,
- significant aerodynamic cross-coupling



(a) Damping derivatives. Wing-body-fin configuration $M = 0.7$. NAE



(b) Low subsonic yawing moment and damping derivatives. Current fighter configuration. (Ref. 9)



(c) Low subsonic cross derivatives. Swept-wing fighter configuration. (Ref. 10)

Figure 4. Examples of non-linearities in damping and cross derivatives.

between the lateral and the longitudinal degrees of freedom,

- time-dependent effects,
- strong configuration dependence,
- need for more sophisticated mathematical modelling.

3.1 Non-Linearities

Large variations with the angle of attack of the various complex flow features discussed in the previous section frequently cause significant non-linearities in the stability parameters. Instead of being constants, as is normally the case at zero or low angles of attack, these parameters now display large variations with angle of attack and are also known to be dependent on the angle of sideslip and, in appropriate cases, also on the rate of spin.

Some examples of these non-linearities are presented in Fig. 4. In the top row, the three damping derivatives are shown, as measured at NAE for a wing-body configuration at a Mach number of 0.7(7,8). The curves amply illustrate both the magnitude and the suddenness of the variations with angle of attack. It can be appreciated that if the angle of attack about which the oscillation takes place happens to be in the region where a sudden change in a derivative occurs, large effects of the amplitude of oscillation may be expected. This is also often associated with the occurrence of aerodynamic hysteresis. In cases like this the derivative concept can only give an equivalent linearized description of the dependence of the aerodynamic reaction on the variable of motion and a better mathematical formulation may be needed.

Non-linear effects were also measured at NASA Langley for fighter aircraft at low subsonic speeds(9). In Fig. 4(b), the non-linear variation of the yawing moment with the rate of rotation in a right spin is shown. Positive values of C_n contribute to the driving moment in the spin and correspond to positive (destabilizing) values of the yaw damping derivative. Also shown are very sudden and large unstable peaks in two of the damping derivatives. Of particular interest is the very large dependence of the roll damping derivative on the amplitude of oscillation at angles of attack between 25° and 45°. The smaller the amplitude of oscillation, the more pronounced is the local instability in roll. It has also been observed (although not shown here) that a decreasing oscillation frequency has a similar destabilizing effect, indicating that the governing factor for this phenomenon is the maximum angular velocity in roll experienced by the aircraft. This effect, which is usually the result of flow separation and loss of lift on the downward wing, is often responsible for the occurrence of wing rock.

Equally dramatic non-linearities with angle of attack occur also in other dynamic derivatives, such as the familiar cross derivatives(10) between the rolling and yawing degrees of freedom shown at the bottom of Fig. 4. It is interesting to note from Ref. 10 that the angle of attack at which these peaks occur is largely independent of both the wing sweep angle and the presence of vertical tails. This suggests that the primary mechanism for these effects is associated with the existence and motion of the forebody vortices.

3.2 Aerodynamic Cross-Coupling

As discussed in Section 2, asymmetric flow conditions may occur not only when an aircraft flies at non-zero angle of sideslip but also when it flies at zero sideslip but at high angles of attack. If, in addition, the aircraft is performing an oscillatory motion in pitch, the asymmetric flows will oscillate to and fro, giving rise - because of various lag effects - to lateral aerodynamic reactions that will have components both in phase

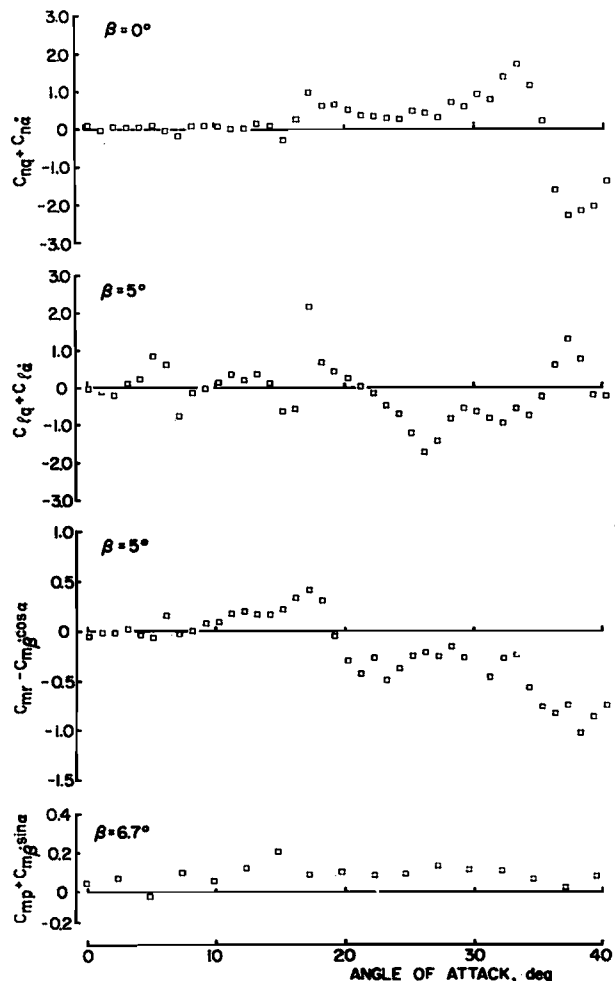


Figure 5. Examples of dynamic cross-coupling derivatives. (Wing-body-fin configuration, M = 0.7.)
NAE

and out of phase with the pitching oscillation of the aircraft. Similarly - once the asymmetry is introduced - there will be longitudinal reactions both in phase and out of phase with the lateral oscillation of the aircraft. In the first approximation, such effects can be described in terms of the static and dynamic *cross-coupling* derivatives, referring this term to the aerodynamic cross coupling between the longitudinal and the lateral degrees of freedom of the aircraft (and reserving the term *cross* derivatives for the traditional derivatives that relate two lateral degrees of freedom, such as roll and yaw). The introduction of cross-coupling derivatives requires simultaneous consideration of *all* the equations of motion of an aircraft, rather than of separate groups of equations for the longitudinal and for the lateral motions, as often done in the past.

The concept of aerodynamic cross-coupling, especially in relation to the dynamic stability derivatives, was introduced only relatively recently(11). New experimental capabilities had to be developed to permit the measurement of the pertinent derivatives. Some of these new apparatuses are briefly described in Section 4. So far, only relatively few measurements of this kind have been performed. Some examples of the dynamic cross-coupling derivatives obtained on simple wing-body-fin configurations(8,12) are given in Fig. 5. From top to bottom, the dynamic yawing and rolling moment derivatives due to oscillation in pitch are shown, followed by the dynamic pitching moment derivatives due to oscillations in yaw and in roll. The angle of sideslip in these examples varies. In all cases, the derivatives are relatively small for low angles of attack but attain large values and display sudden variations at angles of attack between 15° and 20°, and - except for the bottom example, which was obtained for a slightly different configuration - become quite irregular at higher angles of attack, especially in the region between 32° and 38°. Both the levels attained and the suddenness of variations is larger for the derivatives of the lateral moments due to oscillation in pitch than for the pitching moment derivatives due to oscillations in yaw and in roll. It should be noted that these cross-coupling derivatives may be of the same order, and sometimes even larger, than the corresponding traditional damping derivatives (except for the damping-in-pitch derivatives at high angles of attack), such as previously shown in Figure 4. The same conclusion can also be reached when comparing, instead of the derivatives, the corresponding terms in the pertinent equations of motion(7,13).

As can be expected from basic aerodynamic considerations, the direct and the cross derivatives should be symmetrical with respect to zero angle of sideslip,

whereas the cross-coupling derivatives should change sign with the direction of sideslip. This is demonstrated in Fig. 6, where the three dynamic moment derivatives due to oscillation in roll are plotted as functions of the angle of sideslip. The antisymmetric variation of the cross-coupling derivative with the angle of sideslip is clearly visible. Another example of such a variation is given in Fig. 9 of Ref. 7.

The importance of including - at high angles of attack - the aerodynamic cross-coupling terms in the equations of motion has been studied, on a hybrid(13) or a fully digital(14) computer, by examining the sensitivity to these terms of the predicted motion time histories. Fig. 7 shows the angular rates resulting from a sudden perturbation in α of 0.05 rad. for a hypothetical military aircraft in a 2 g turning flight. Had the dynamic cross-coupling terms not been included, the rates p , r and β would have remained essentially constant. It was shown in these studies that the dynamic derivatives of the two lateral moments due to oscillation in

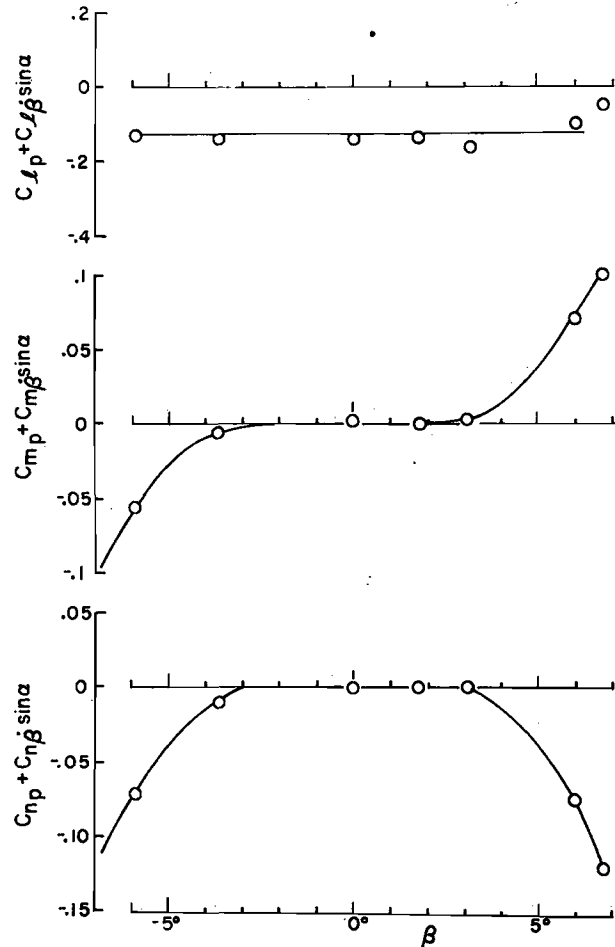
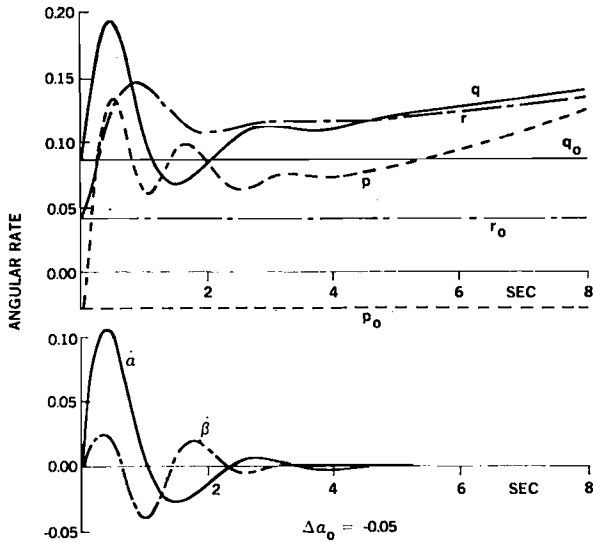


Figure 6. Effect of sideslip on dynamic moment derivatives due to oscillation in roll. $M = 0.7$, $\alpha = 17.5^\circ$.

NAE



NOTE 1: ANGULAR RATES FOR THE UNPERTURBED CASE REMAIN CONSTANT AND ARE DENOTED BY p_0, q_0, r_0 .

NOTE 2: WITH ALL AERODYNAMIC CROSS COUPLING DERIVATIVES EQUAL TO ZERO, THE RATES $p, r,$ AND $\dot{\beta}$ REMAIN ESSENTIALLY CONSTANT WHEN PERTURBED IN α .

Figure 7. Effect of dynamic cross-coupling terms for a military aircraft in 2 g turning flight. Locally linearized coefficients; $\alpha = 33^\circ$. (Ref. 13)

pitch were particularly significant and in some cases could have an effect on the predicted motion that could be as large as that of some of the well-known damping and cross derivatives.

3.3 Time-Dependent Effects

In addition to *quasi-steady* effects, such as represented by derivatives of various aerodynamic reactions due to angular velocities, we have to consider the existence of purely *unsteady* effects, such as those represented by derivatives due to the time rate of change of angular deflections, $\dot{\alpha}$ or $\dot{\beta}$. These derivatives have been known for many years, since they constitute part of the dynamic results obtained with standard wind-tunnel techniques of oscillation around a fixed axis, which always give composite derivative expressions such as $(C_{mq} + C_{m\dot{\alpha}})$. Up to now, however it was standard practice to ignore the $\dot{\alpha}$ and $\dot{\beta}$ effects (or to introduce a simple correction for them) and to use the composite derivatives in place of the purely rotary ones. At low angles of attack the error introduced by such a procedure was often small and the simplification large enough to be justifiable.

At higher angles of attack, however, the $\dot{\alpha}$ and $\dot{\beta}$ effects unfortunately become quite substantial and can no longer be ignored or corrected for in a simple fashion. This is illustrated in Fig. 8, where

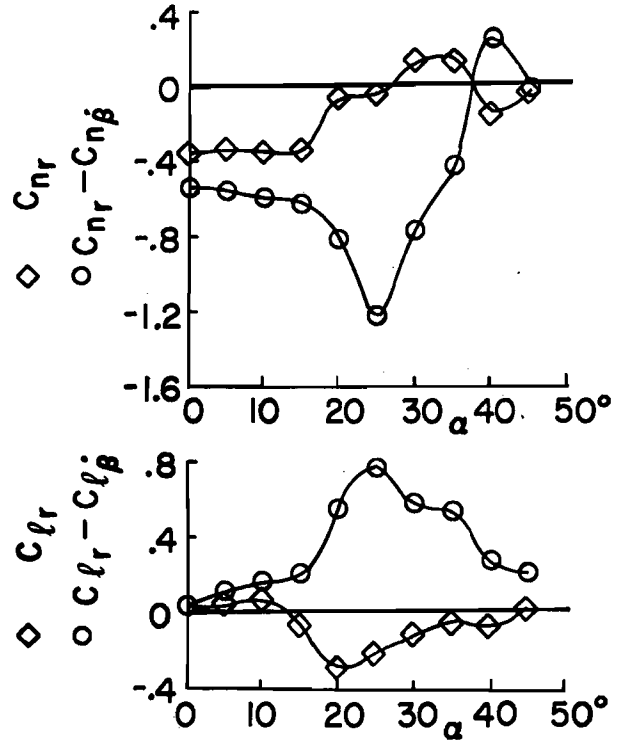


Figure 8. $\dot{\beta}$ -derivatives obtained as difference between purely rotary and oscillatory derivatives. (Ref. 15)

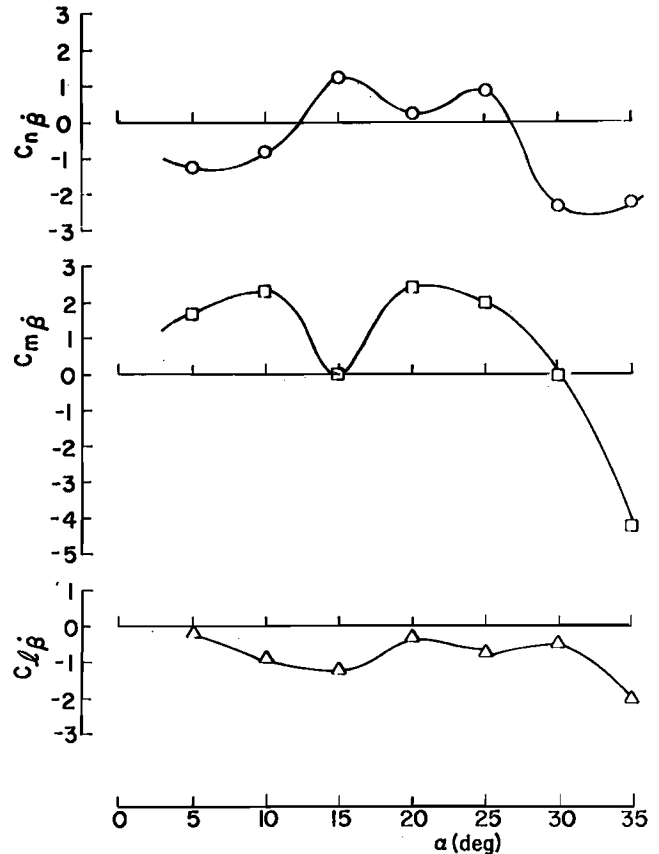
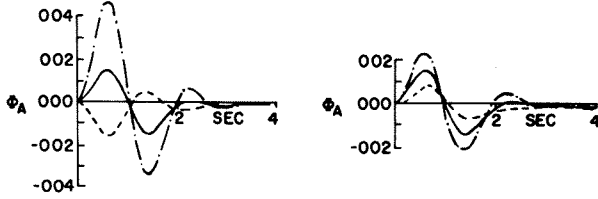


Figure 9. $\dot{\beta}$ -derivatives measured directly (preliminary data). NAE

C_{l_q} AND $C_{l_{\dot{\alpha}}}$ LEGEND C_{l_q} $C_{l_{\dot{\alpha}}}$
 ZERO - - - - ZERO TWICE NOMINAL
 NOMINAL - - - NOMINAL NOMINAL
 TWICE NOMINAL - - - - TWICE NOMINAL ZERO



LOCALLY LINEARIZED COEFFICIENTS; $\Delta\alpha_0 = -0.05$

Figure 10. Relative importance of $C_{l_q} + C_{l_{\dot{\alpha}}}$, C_{l_q} and $C_{l_{\dot{\alpha}}}$. Same conditions as in Figure 7. (Ref. 13)

the composite derivatives obtained from oscillatory experiments around a fixed axis are compared with purely rotary derivatives obtained from experiments in a curved flow⁽¹⁵⁾. The difference between the two sets of results represents the unsteady effects due to the time rate of change of the angular deflection (in this case of the angle of sideslip) and becomes quite significant for higher angles of attack.

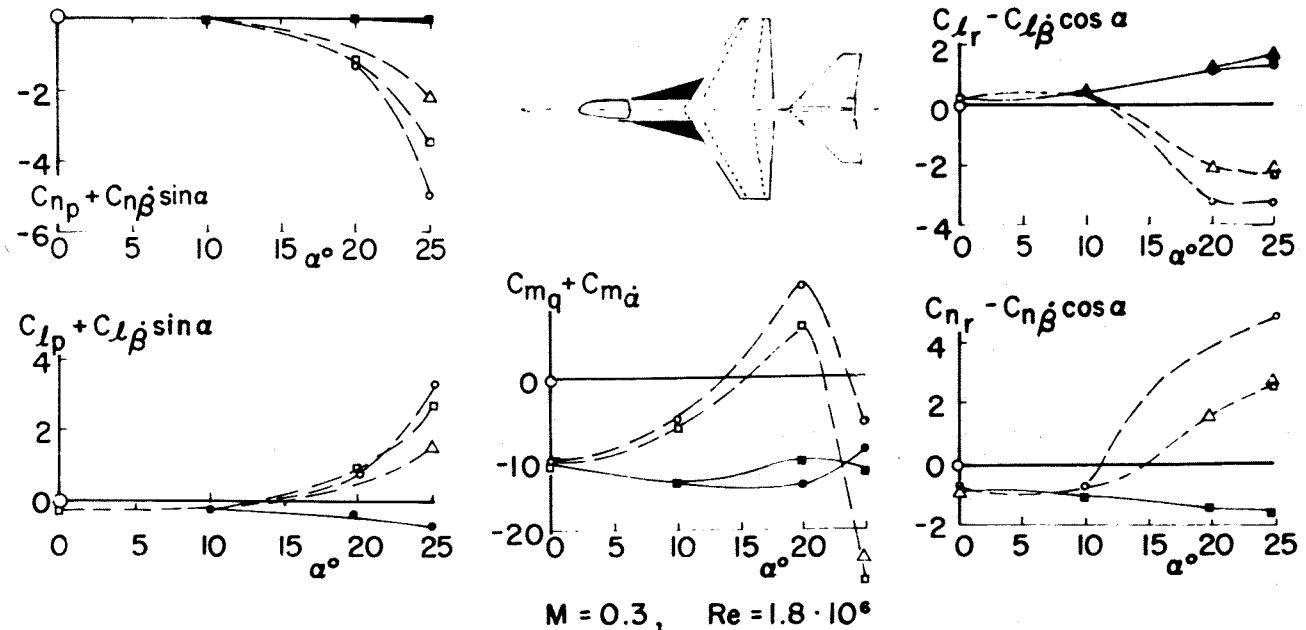
Derivatives due to the time rate of change of angular deflections are aerodynamically equivalent (in the first

approximation) to derivatives due to translational acceleration in the same plane of motion. This fact renders them of high interest for aircraft designs using direct-lift or direct side-force controls and also makes it possible to determine them experimentally using a translational oscillatory motion in the vertical or lateral direction. An example of β -derivatives measured in a lateral-oscillation experiment⁽¹⁶⁾ is shown in Fig. 9 (preliminary data).

It was demonstrated in the aforementioned sensitivity studies^(13,14), that using the sum of the rotary and the acceleration derivatives in lieu of the rotary ones alone, or even considering these two parts at their proper place in the equations of motion but arbitrarily making them equal in magnitude, may lead to significant errors. This is illustrated in Fig. 10, where the predicted time history of the aerodynamic roll angle is shown for the various combinations of derivatives C_{l_q} and $C_{l_{\dot{\alpha}}}$ for the same conditions as in Fig. 7.

3.4 Configuration Dependence

The intricate vortex pattern that exists around an aircraft configuration at high angles of attack is very sensitive to even small changes in aircraft geometry.



$\frac{p \cdot b}{2V}$	STRAKE OFF	STRAKE ON	$\frac{q \cdot c}{V}$	STRAKE OFF	STRAKE ON	$\frac{r \cdot b}{2V}$	STRAKE OFF	STRAKE ON
0.047	---○---	---●---	0.03	---○---	---●---	0.05	---○---	---●---
0.057	---□---	---■---	0.038	---□---	---■---	0.062	---□---	---■---
0.07	---△---	---▲---	0.047	---△---	---▲---	0.068	---△---	---▲---

ROLLING

PITCHING

YAWING

Figure 11. Effect of strakes on dynamic derivatives of a current aircraft configuration. MBB-ONERA (Ref.17)

So is the behaviour of this vortex pattern on an oscillating configuration. The forebody vortices are greatly dependent on the planform and the cross-sectional geometry of the aircraft nose as well as on the presence of various forms of protuberances on the forebody that may affect the stability of an existing vortex pattern, give rise to new vortices and create conditions for strong vortex interactions. The wing leading-edge vortices, in addition to being a strong function of the leading edge sweep as discussed before, are also known to be greatly affected by various leading-edge modifications, such as apex drooping, discontinuities or contouring, and by various modifications of the wing itself, such as addition of wing leeside fences and deflection of leading-edge or trailing-edge flaps. All these variations of the geometry of a wing affect not only the position and the strength of the wing vortices but also the all-important location at which these vortices break down(4).

The most common modification of the aircraft geometry intended to eliminate or to delay the onset of asymmetric effects is the use of forebody strakes. These strakes are often combined with leading edge extensions (theso-called LEX) or with some suitable modifications of the shape of the forebody (usually by flattening and broadening the nose). An illustration of

a successful application of such strakes (or LEX) is given in Fig. 11, where the three damping and the two cross derivatives are shown for a configuration with and without strakes(17). In all cases the addition of strakes reduces the magnitude of the derivatives, decreases the non-linearities with angle of attack and makes the derivatives less dependent on the reduced frequency. The dynamic cross derivative of the yawing moment due to rolling becomes essentially zero. The negative dampings in roll, in pitch and in yaw completely disappear. It should be noted, however, that the range of angle of attack investigated extends only to $\alpha = 25^\circ$, and that the results have been obtained for only four values of α , leaving the possibility of existence of undetected peaks (for instance, between $\alpha = 10^\circ$ and $\alpha = 20^\circ$).

As is well-known, however, strakes do have certain disadvantages. Their successful development for a particular application may require several design iterations. They often adversely affect the directional stability. If mounted near the tip of the nose radome, they may disturb the radar operations. The strake vortices may adversely interact with aircraft components further downstream, such as air intakes or control surfaces. Therefore, it may not always be possible to use strakes, and other approaches (such as the use of

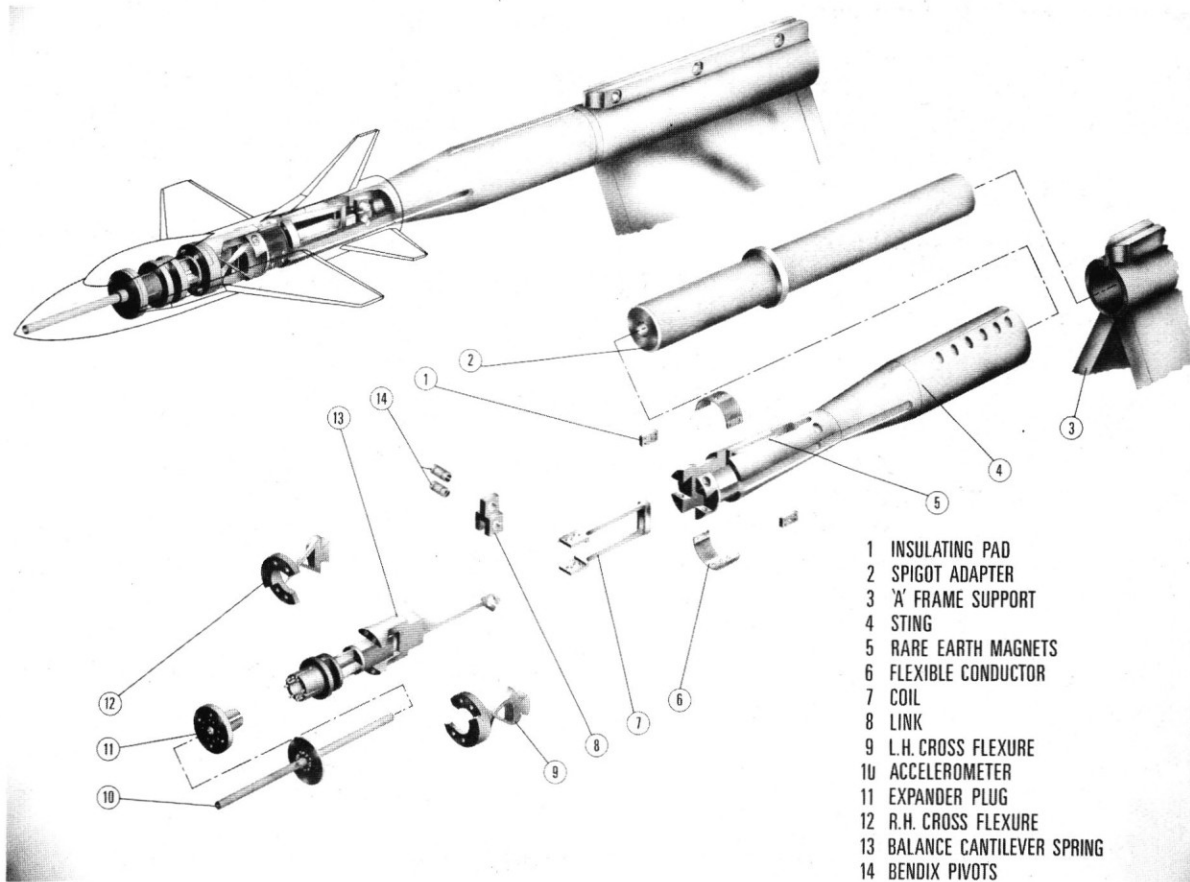


Figure 12. Exploded view of the new pitch/yaw oscillation apparatus.
NAE

helical trips or jet injection on the forebody) continue to be of high interest.

It should be noted that both strakes and helical trips, if used in single pairs, rapidly lose efficiency as the banking angle increases; such devices would therefore be of little use on bodies which have to rotate in roll at high angles of attack, such as certain missiles and projectiles.

3.5 Mathematical Modelling

The mathematical modelling used in most countries at the present time to describe the aircraft flight history applies strictly to flight at small to moderate angles of attack, where nonlinearities are small, time-dependent effects insignificant, and aerodynamic cross-coupling non-existent. A much more sophisticated modelling, which would include all the above effects, is obviously required for a satisfactory description of flight at high angles of attack. In addition, at very high angles of attack, a satisfactory representation of spinning or coning is also required.

Substantial progress has already been made in some of these areas. A generalized formulation which includes the nonlinear pitch-yaw-roll coupling and nonlinear coning rates is now available (18). Time-history effects have recently been included in that formulation (19). Among things still to be done is an adequate modelling of the suddenness with which the aerodynamic reactions may vary with the angle of attack or sideslip, and a satisfactory verification of some of the more advanced mathematical models. The verification should be conducted by determining a complete set of stability parameters for a particular configuration, by predicting a series of rather extreme maneuvers and by comparing them with the actual flight histories. One of the principal difficulties in conducting such a verification at the present time is the lack of complete static and dynamic aerodynamic data for the required test cases.

4. NEW DYNAMIC-STABILITY TEST TECHNIQUES

As already indicated, the determination of the additional dynamic stability

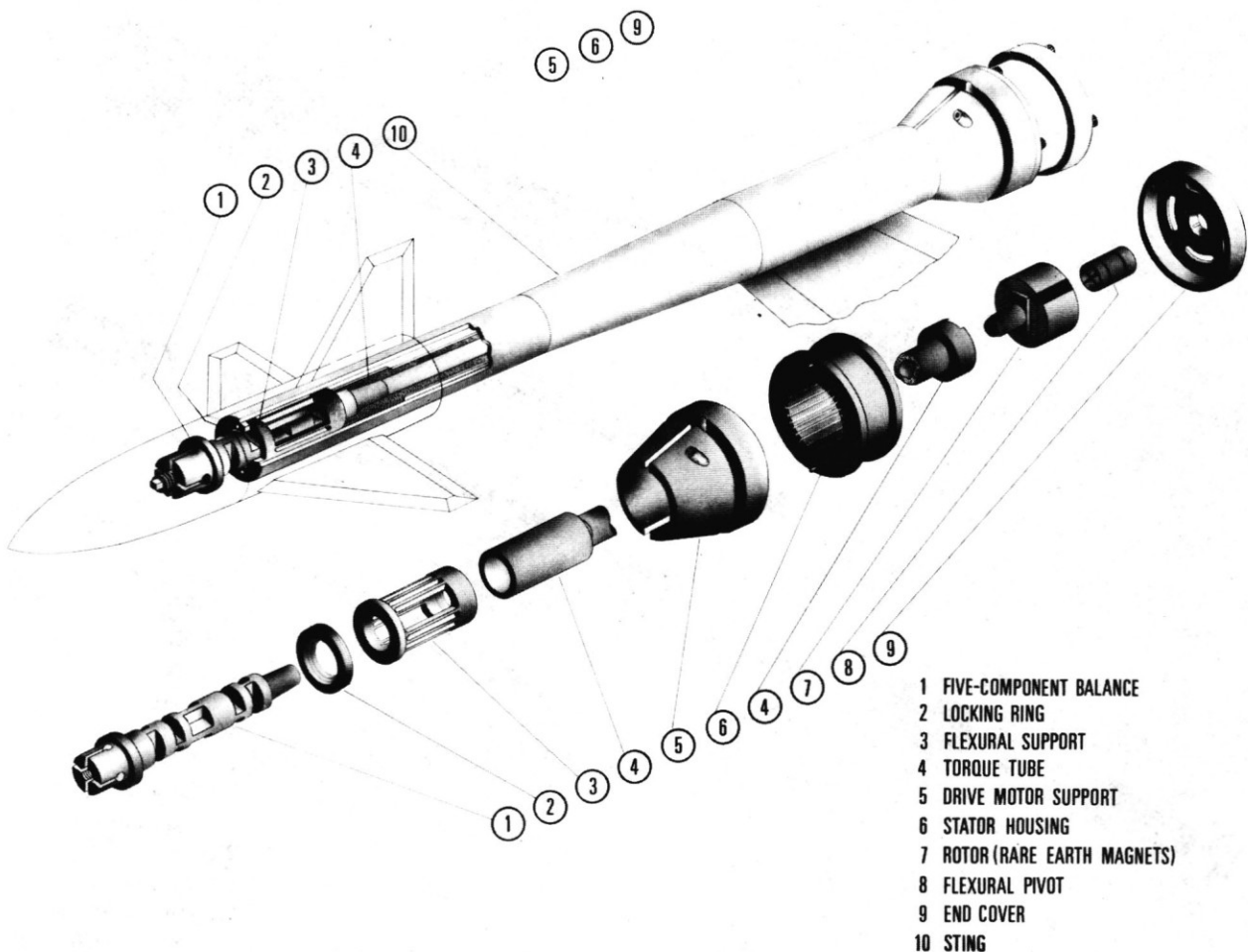


Figure 13. Exploded view of the roll oscillation apparatus.
 NAE

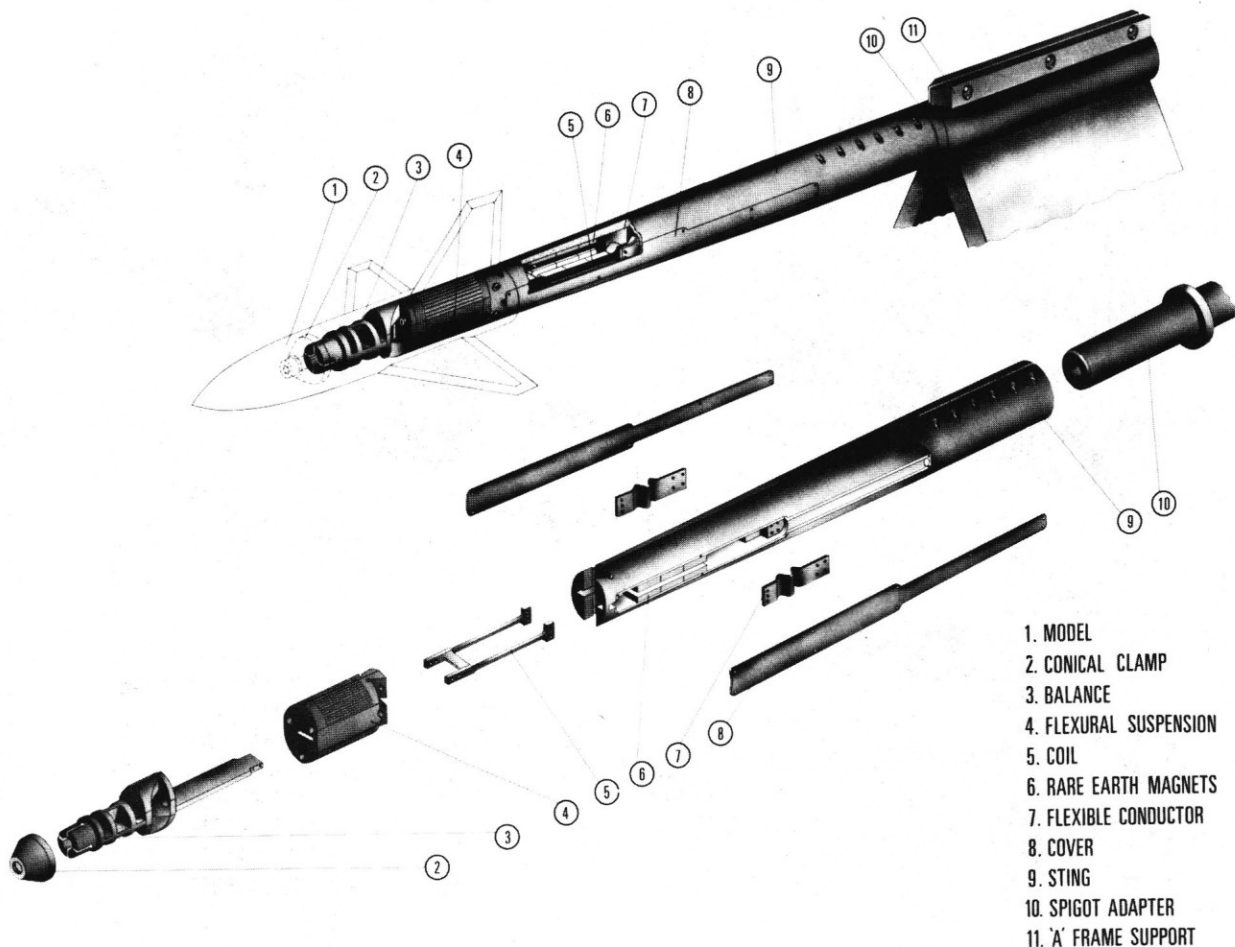
data that are associated with flight at high angles of attack requires the availability of novel test techniques with greatly expanded capabilities. These should include the capabilities

- to test at high angles of attack, and to carry the associated high loads,
- to measure dynamic cross coupling derivatives,
- to measure effects due to $\dot{\alpha}$ and $\dot{\beta}$,
- to measure effects due to coning and continuous rolling,
- to test at large amplitude of oscillation, particularly in the case of oscillation in roll.

A fairly complete review of existing testing techniques for determination of dynamic stability parameters in a wind tunnel was given in Ref. 20, with additional information available elsewhere in Ref. 6. Since that time significant developments have taken place at several establishments in various countries of the world, notably so at NASA Ames, NASA Langley, AEDC, RAE Bedford, BAC Warton, DFVLR and ONERA. Due to space limitations it is impossible to include any discussion

of these developments in the present paper; instead a brief account will be rendered of the techniques presently available at the National Aeronautical Establishment in Ottawa. Although the NAE techniques do not yet include capabilities for coning or large amplitude oscillation, they do satisfy the remaining three of the five requirements listed above and must be considered, therefore, as fairly representative of the new experimental trends in this field.

In Table 1 a list is presented of the presently available three full-model and two half-model apparatuses that can be used to study the primary oscillations in 5 degrees of freedom, providing means to determine all the moment derivatives and some of the force derivatives associated with these motions. Both static and dynamic derivatives are included and the list encompasses the direct, cross and cross-coupling derivatives, as discussed before. It should be noted that in all cases the derivatives are obtained from a *direct* measurement, which is based only on an assumed relation between the aerodynamic reaction measured and the causative primary motion. Often this relation is linear,



1. MODEL
2. CONICAL CLAMP
3. BALANCE
4. FLEXURAL SUSPENSION
5. COIL
6. RARE EARTH MAGNETS
7. FLEXIBLE CONDUCTOR
8. COVER
9. STING
10. SPIGOT ADAPTER
11. 'A' FRAME SUPPORT

Figure 14. Exploded view of the translational oscillation apparatus.
NAE

APPARATUS	PRIMARY MOTION	STATIC DERIVATIVES	DYNAMIC DERIVATIVES
PITCH/YAW	PITCHING OSCILLATION	C_{Ia}, C_{ma}, C_{na}	$C_{Ia} + C_{Ia}$ $C_{ma} + C_{ma}$ $C_{na} + C_{na}$
PITCH/YAW	YAWING OSCILLATION	$C_{I\beta}, C_{m\beta}, C_{n\beta}$	$C_{I\beta} - C_{I\beta} \cos \alpha$ $C_{m\beta} - C_{m\beta} \cos \alpha$ $C_{n\beta} - C_{n\beta} \cos \alpha$
ROLL	ROLLING OSCILLATION	$C_{I\beta} \sin \alpha$ $C_{m\beta} \sin \alpha$ $C_{n\beta} \sin \alpha$ $C_{Y\beta} \sin \alpha$ $C_{N\beta} \sin \alpha$	$C_{I\beta} + C_{I\beta} \sin \alpha$ $C_{m\beta} + C_{m\beta} \sin \alpha$ $C_{n\beta} + C_{n\beta} \sin \alpha$ $C_{Y\beta} + C_{Y\beta} \sin \alpha$ $C_{N\beta} + C_{N\beta} \sin \alpha$
$\dot{\alpha}/\dot{\beta}$	PLUNGING OSCILLATION	C_{Ia}, C_{ma}, C_{na}	C_{Ia}, C_{ma}, C_{na}
$\dot{\alpha}/\dot{\beta}$	LATERAL OSCILLATION	$C_{I\beta}, C_{m\beta}, C_{n\beta}$	$C_{I\beta}, C_{m\beta}, C_{n\beta}$
PITCH (HALF-MODEL)	PITCHING OSCILLATION	C_{ma}	$C_{mq} + C_{ma}$
PLUNGE (HALF-MODEL)	PLUNGING OSCILLATION	C_{ma}	C_{ma}

Table 1. NAE Dynamic Stability Testing Capabilities.

but can be replaced by a non-linear or higher order formulation, if the need arises. Since the motion is essentially in one degree of freedom, the measurement is independent of the remaining parts of the equations of motion and therefore the results may be expected to be valid for any formulation of these equations as long, of course, as the principle of superposition is still applicable, that is as long as the concept of stability derivatives can be used.

Figs. 12, 13 and 14 show the new NAE pitch/yaw apparatus, just being completed, the roll apparatus(8) and the translational oscillation apparatus(16), respectively. In all cases the model is mounted on a balance that in turn is attached to an elastic support system capable of deflecting in the appropriate degree of freedom. The primary motion is imparted by an electro-magnetic drive mechanism which oscillates the model with a constant amplitude at the resonance frequency in the primary degree of freedom. Each balance has a multi-component capability (but always without axial force) and is made in

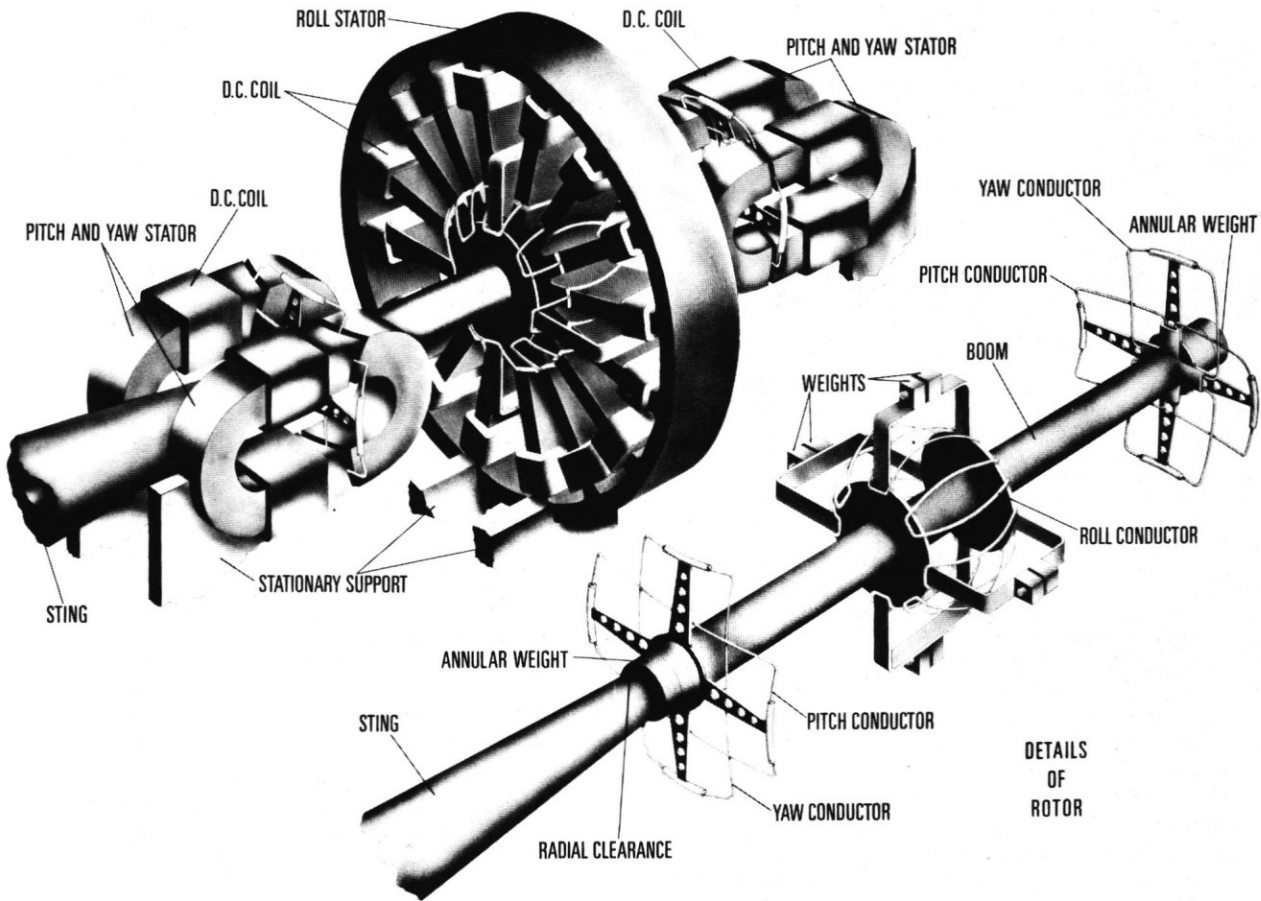


Figure 15. Pictorial view of the new 3 DOF dynamic calibrator. NAE

one piece - a most desirable feature for dynamic testing. Each drive mechanism utilizes a high-current coil (or coils) moving in a strong magnetic field that is generated by compact rare-earth permanent magnets. As a result, the apparatuses are relatively slender and permit testing of realistic models of current aircraft configurations.

The high complexity of the aforementioned techniques and the lack of any previous data on some of the recently identified dynamic derivatives made it necessary to develop a system that would independently verify the validity of the experimental technique and data-reduction methods employed. The same system was also conceived as a diagnostic tool to identify, on a regular basis, equipment faults or software errors. A pictorial view of such a system developed at NAE and called a *dynamic calibrator* (21), is shown in Fig. 15. The aircraft model is replaced on the dynamic stability apparatus by a special calibrating frame (or "rotor"), which is then oscillated in the primary degree of freedom by the drive mechanism of the apparatus. The inertia characteristics of the rotor duplicate, at least approximately, the inertia characteristics of the model, resulting in a similar dynamic response of the rotor and of the model in all three degrees of freedom. The three oscillatory aerodynamic moments, acting on the oscillating model during a wind tunnel test, are simulated by accurately known, electromagnetically induced, *alternating* loads, whose phase and amplitude can be adjusted at will. A comparison between the known applied loads and the outputs of the dynamic stability apparatus, obtained by processing the balance data and other relevant information by means of the same procedure as in the wind tunnel experiments, provides an overall calibration of the technique and all the mechanical and electronic systems involved. Other dynamic calibrators, simpler but based on similar principles, have been developed for half-model dynamic apparatuses.

5. FUTURE GOALS

A brief review has been presented of the potentially important dynamic stability problems that may be associated with the high angle-of-attack flight conditions, and a brief summary has been given of the initial attempts that have been made to date to better understand and identify these problems. More work is necessary in this entire field of studies and, in particular, increased attention is urgently required in the following areas:

- fluid dynamics of the oscillatory flow phenomena at high angles of attack and their effect on dynamic stability parameters;
- mathematical modelling of the aerodynamics of high angle-of-attack maneuvers with proper accounting of the

non-linear, cross-coupling and time-dependent effects;

- determination of complete sets of stability parameters for at least one advanced configuration, in order to make the new modelling and its verification (by comparison with flight histories) possible;
- effects of wind-tunnel and support interference on the required oscillatory experiments at high angles of attack;
- control derivatives;
- stability parameters of aeroelastic configurations.

It is hoped that this review paper may perhaps be instrumental in triggering a response and some intensified action in one or more of these areas.

6. REFERENCES

1. High angle of attack aerodynamics. Proc. of FDP Symposium in Sandefjord, Norway, AGARD CP-247, 1978.
2. Peake, D.J. and Tobak, M. Three-dimensional interactions and vortical flows with emphasis on high speeds. NASA TM 81169, 1980; also AGARDograph 252, 1980.
3. Chapman, G.T., Keener, E.R. and Malcolm, G.N. Asymmetric aerodynamic forces on aircraft forebodies at high angles of attack - some design guides. AGARD CP-199, Paper 12, 1975.
4. Erickson, G.E. Water tunnel flow visualization: Insight into complex three-dimensional flow fields. AIAA 79-1530, 1979.
5. Keener, E.R. and Chapman, G.T. Similarity in vortex asymmetries over slender bodies and wings. AIAA Journal, Vol. 15, No. 9, 1977.
6. Dynamic stability parameters. Proc. of FDP Symposium in Athens, Greece. AGARD CP-235, 1978.
7. Orlik-Rückemann, K.J. Aerodynamic coupling between lateral and longitudinal degrees of freedom. AIAA Journal Vol. 15, No. 12, 1977.
8. Hanff, E.S., Orlik-Rückemann, K.J., Kapoor, K.B., Moulton, B.E. and LaBerge, J.G. New oscillatory roll apparatus and results on direct, cross and cross-coupling subsonic moment derivatives for an aircraft-like model. NRC NAE LTR-UA-50, 1979.
9. Chambers, J.R., Gilbert, W.P. and Nguyen, L.T. Results of piloted simulator studies of fighter aircraft at high angles of attack. Paper 33 in Ref. 6, 1978.

10. Grafton, S.B. and Anglin, E.L. Dynamic stability derivatives at angles of attack from -5° to 90° for a variable-sweep fighter configuration with twin vertical tails. NASA TN D-6909, 1972.
11. Orlik-Rückemann, K.J. Dynamic stability testing of aircraft - needs versus capabilities. Proc. of Int. Congr. on Instr. in Aerospace Simulation Facilities, ICIAAF '73 Record, pp 8-23, 1973.
12. Orlik-Rückemann, K.J., Hanff, E.S. and LaBerge, J.G. Direct and cross-coupling subsonic moment derivatives due to oscillatory pitching and yawing of an aircraft-like model at angles of attack up to 40° in Ames 6'x6' wind tunnel. NRC NAE LTR-UA-38, 1976.
13. Curry, W.H. and Orlik-Rückemann, K.J. Sensitivity of aircraft motion to aerodynamic cross-coupling at high angles of attack. Paper 34 in Ref. 6, 1978.
14. Butler, R.W. and Langham, T.F. Aircraft motion sensitivity to variations in dynamic stability parameters. Paper 35 in Ref. 6, 1978.
15. Coe, P.L., Jr. and Newson, W.A. Jr. Wind-tunnel investigation to determine the low-speed yawing stability derivatives of a twin-jet fighter model at high angles of attack. NASA TN D-7721, 1974.
16. Orlik-Rückemann, K.J., Hanff, E.S. and Anstey, C.R. Wind-tunnel apparatus for translational-oscillation experiments. AIAA 18th Aerospace Sciences Meeting, AIAA 80-0046, 1980.
17. Staudacher, W., Laschka, B., Schulze, B., Poisson-Quinton, P. and Canu, M. Some factors affecting the dynamic stability derivatives of a fighter-type model. Paper 11 in Ref. 6, 1978.
18. Tobak, M. and Schiff, L.B. On the formulation of the aerodynamic characteristics in aircraft dynamics. NASA TR R-456, 1976.
19. Tobak, M. and Schiff, L.B. The role of time-history effects in the formulation of the aerodynamics of aircraft dynamics. Paper 26 in Ref. 6, 1978.
20. Orlik-Rückemann, K.J. Techniques for dynamic stability testing in wind tunnels. Paper 1 in Ref. 6, 1978.
21. Hanff, E.S. An advanced calibrator for dynamic wind-tunnel experiments. Proc. of the 25th ISA International Instrumentation Symposium, pp. 239-244, 1979.